

Drag Reduction in Homogeneous Turbulence by Scale-Dependent Effective Viscosity

Roberto Benzi^{1,2}, Emily S.C. Ching², and Itamar Procaccia^{2,3}

¹ Dip. di Fisica and INFN, Università “Tor Vergata”,
Via della Ricerca Scientifica 1, I-00133 Roma, Italy,

²Dept. of Physics, The Chinese University of Hong Kong, Shatin, Hong Kong,

³ Dept. of Chemical Physics, The Weizmann Institute of Science, Rehovot, 76100 Israel.

The phenomenon of drag reduction by polymer additives had been studied in simulations on the basis of non-Newtonian fluid mechanical models that take into account the field of polymer extension (conformation tensor) and its interaction with the velocity field. Drag reduction was found in both homogeneous and wall bounded turbulent flows. In the latter case it was shown recently that the notion of scale-dependent effective viscosity allows quantitative predictions of the characteristics of drag reduction in close correspondence with experiments. In this paper we demonstrate that also drag reduction in homogeneous turbulence is usefully discussed in terms of a scale-dependent viscosity. In other words, the essence of the phenomena under study can be recaptured by an “equivalent” equation of motion for the velocity field alone, with a judiciously chosen scale-dependent effective viscosity that succinctly summarizes the important aspects of the interaction between the polymer conformation tensor field and the velocity field. We will also clarify here the differences between drag reduction in homogeneous and wall bounded flows.

I. INTRODUCTION

The addition of long chained polymers to turbulent flows can result in a significant reduction in the drag [1, 2, 3, 4]. The phenomenon had been discovered in 1949 [5] and had since attracted large amount of attention, with much of the experimental literature reviewed and systematized by Virk [3]; the amount of drag depends on the characteristics of the polymer and its concentration, but cannot exceed an asymptote known as the “Maximum Drag Reduction” curve which is independent of the polymer’s concentration or its characteristics. The understanding of this phenomenon had seen significant progress recently. A first step in forming a new understanding were direct numerical simulations of model equations of viscoelastic flows, both in wall bounded and in homogeneous turbulence [6, 7, 8]. The Oldroyd-B and the FENE-P models first, and then simplified models like shell models and Burger’s like models [9, 10, 11], all exhibited drag reduction as a result of including the interaction between the velocity field and a second field representing the polymer (end-to-end) conformation tensor, see Figs. 1 and 2. In homogeneous turbulence drag reduction is exhibited as the increase in the root-mean-square (rms) velocity fluctuations at scales larger than the Lumley scale defined as the scale for which the eddy turnover time is of the order of the polymer relaxation time. The intermediate scale rms energy fluctuations are suppressed due to transfer of energy to the polymers. In wall bounded turbulence drag reduction entails an increase in the mean velocity for a given pressure head, see Fig. 1. Here the Reynolds stress at the intermediate scales is suppressed [12]; we will argue however that there is a difference between the increase in the rms velocity fluctuations at large scales in homogeneous flows and the increase in mean velocity in wall bounded flows; the former disappears when the system size goes to in-

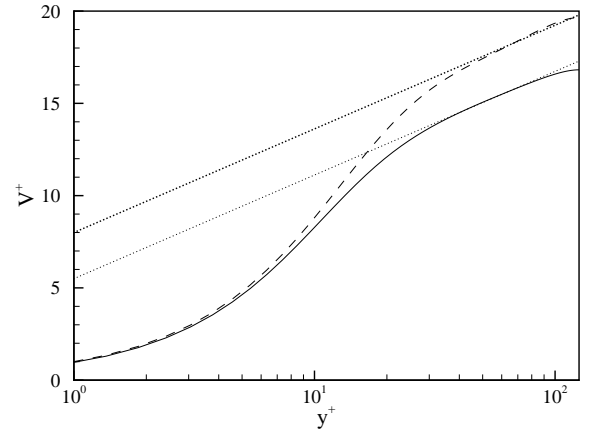


FIG. 1: Mean velocity profile of the FENE-P (dashed line) and of the Navier-Stokes equations (solid line) in wall bounded channel flow as a function of the reduced distance from the wall. The relative increase of the mean velocity (indicated by the asymptotic straight lines) is the phenomenon of drag reduction in wall bounded flows.

finity (for a fixed Lumley scale). In the latter case an increase in the mean velocity near the wall (small and intermediate scales) does not disappear with increasing the system’s size. This difference is fundamental to the different symmetries at play, the Galilean invariance in the case of the wall bounded flow vs. translational invariance in the case of homogeneous flows. Nevertheless we will argue below that the two cases can be discussed in similar physical terms. In a recent paper it was shown that drag reduction in wall bounded flows can be conveniently discussed in terms of a ‘scale-dependent’ effective viscosity. The aim of the present paper is to demonstrate that this notion is also useful in the context of homogeneous

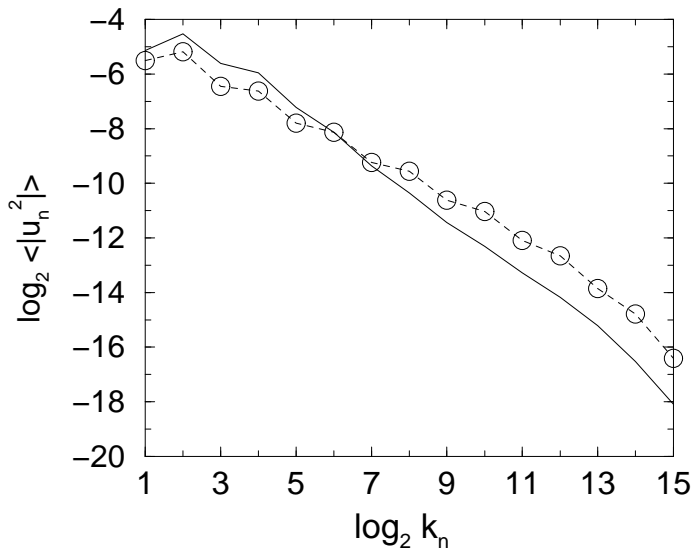


FIG. 2: Energy spectrum of the SabraP model (line) and the Sabra model (dashed line with symbols) for $\nu = 10^{-7}$. The relative increase of the energy spectrum at small values of n is the phenomenon of drag reduction in homogeneous turbulence in general and in shell models in particular, see Sect. III for details.

turbulence. In doing so we aim at simplifying the theoretical description, eliminating the explicit presence of a second field in the equations of motion, leaving the velocity field alone. The eliminated field, which represents the conformation tensor of the polymers, remains only as an effective viscosity in the equation of motion. Needless to say, this effective viscosity cannot be a number, since the amount of energy transferred from the velocity field to the polymer is strongly scale dependent; in homogeneous turbulence this transfer achieves a maximum near the Lumley scale. In wall bounded flows the degree of interaction between the polymers and the velocity field is a strong function of the distance from the wall, and so is therefore the effective viscosity. Of course, in a full theory a scale-dependent scalar viscosity is not sufficient either, due to the anisotropy of the polymer end-to-end extension tensor. We would like to demonstrate however that at least in the model equations a surprising proportion of the essential physics can be captured in terms of a simple notion of a scale-dependent viscosity which surrogates the existence of the second field. This thinking goes back to some observations a few years ago regarding the importance of space-dependent viscosity even in the stability of laminar flows [14, 15]. In Sect. 2 we review the two-field models in which drag reduction had been demonstrated in numerical simulations. In Sect. 3 we present the reduction to velocity-alone models with scale-dependent viscosity. In Sect. 4 we present a discussion of the large system size limit and underline the difference between homogeneous and wall bounded flows. Sect. 5 is dedicated to a short summary and conclusions.

II. SHELL MODEL FOR DRAG REDUCTION IN HOMOGENEOUS TURBULENCE

Viscoelastic flows are represented well by hydrodynamic equations in which the effect of the polymer enters in the form of a “conformation tensor” $\mathbf{R}(\mathbf{r}, t)$ which stems from the ensemble average of the dyadic product of the end-to-end distance of the polymer chains [19, 20]. A successful model that had been employed frequently in numerical simulations of turbulent channel flows is the FENE-P model. Flexibility and finite extendability of the polymer chains are reflected by the relaxation time τ and the Peterlin function $P(\mathbf{r}, t)$ which appear in the equation of motion for \mathbf{R} :

$$\frac{\partial R_{\alpha\beta}}{\partial t} + (\mathbf{u} \cdot \nabla) R_{\alpha\beta} = \frac{\partial u_\alpha}{\partial r_\gamma} R_{\gamma\beta} + R_{\alpha\gamma} \frac{\partial u_\beta}{\partial r_\gamma} - \frac{1}{\tau} [P(\mathbf{r}, t) R_{\alpha\beta} - \rho_0^2 \delta_{\alpha\beta}] \quad (1)$$

$$P(\mathbf{r}, t) = (\rho_m^2 - \rho_0^2) / (\rho_m^2 - R_{\gamma\gamma}) \quad (2)$$

In these equations ρ_m^2 and ρ_0^2 refer to the maximal and the equilibrium values of the trace $R_{\gamma\gamma}$. Since in most applications $\rho_m \gg \rho_0$ the Peterlin function can also be written approximately as $P(\mathbf{r}, t) \approx (1/(1 - \alpha R_{\gamma\gamma}))$ where $\alpha = \rho_m^{-2}$. In its turn the conformation tensor appears in the equations for the fluid velocity $\mathbf{u}(\mathbf{r}, t)$ as an additional stress tensor:

$$\frac{\partial \mathbf{u}}{\partial t} + (\mathbf{u} \cdot \nabla) \mathbf{u} = -\nabla p + \nu_s \nabla^2 \mathbf{u} + \nabla \cdot \mathcal{T} + \mathbf{F}, \quad (3)$$

$$\mathcal{T}(\mathbf{r}, t) = \frac{\nu_p}{\tau} \left[\frac{P(\mathbf{r}, t)}{\rho_0^2} \mathbf{R}(\mathbf{r}, t) - \mathbf{1} \right]. \quad (4)$$

Here ν_s is the viscosity of the neat fluid, \mathbf{F} is the forcing and ν_p is a viscosity parameter which is related to the concentration of the polymer, i.e. $\nu_p/\nu_s \sim \Phi$ where Φ is the volume fraction of the polymer. We note however that the tensor field can be rescaled to get rid of the parameter ρ_m^2 in the Peterlin function, $\tilde{R}_{\alpha\beta} = \alpha R_{\alpha\beta}$ with the only consequence of rescaling the parameter ρ_0 accordingly. Thus the actual value of the concentration is open to calibration against the experimental data. These equations were simulated on the computer in a channel or pipe geometry, reproducing faithfully the characteristics of drag reduction in experiments. It should be pointed out however that even for present day computers simulating these equations is quite tasking. It makes sense therefore to try to model these equations further. For the purpose of studying drag reduction in homogeneous systems one can derive a shell model whose simplicity and transparency are assets for analysis and simulations alike. In developing a simple model one is led by the following ideas. First, it should be pointed out that all the nonlinear terms involving the tensor field $\mathbf{R}(\mathbf{r}, t)$ can be reproduced by writing an equation of motion for a vector field $\mathbf{B}(\mathbf{r}, t)$, and interpreting $R_{\alpha\beta}$ as the dyadic product $B_\alpha B_\beta$. The relaxation terms with the Peterlin function are not automatically reproduced this way, and

one needs to add them by hand. Second, we should keep in mind that the above equations exhibit a generalized energy which is the sum of the fluid kinetic energy and the polymer free energy. Led by these consideration the following shell model was proposed in [9, 11]:

$$\begin{aligned} \frac{du_n}{dt} &= \frac{i}{3}\Phi_n(u, u) - \frac{i\nu_p}{3\tau}P(B)\Phi_n(B, B) - \nu_s k_n^2 u_n + F_n, \\ \frac{dB_n}{dt} &= \frac{i}{3}\Phi_n(u, B) - \frac{i}{3}\Phi_n(B, u) - \frac{1}{\tau}P(B)B_n - \nu_B k_n^2 B_n, \\ P(B) &= \frac{1}{1 - \sum_n B_n^* B_n}. \end{aligned} \quad (5)$$

In these equations u_n and B_n stand for the Fourier amplitudes $u(k_n)$ and $B(k_n)$ of the two respective vector fields, but as usual in shell model we take $n = 0, 1, 2, \dots$ and the wavevectors are limited to the set $k_n = 2^n$. The nonlinear interaction terms take the explicit form

$$\begin{aligned} \Phi_n(u, B) &= 3 \left[k_n u_{n+1}^* B_{n+2} + b k_{n-1} u_{n-1}^* B_{n+1} \right. \\ &\quad \left. + (1+b) k_{n-2} u_{n-2} B_{n-1} \right], \end{aligned} \quad (6)$$

with b a parameter and the obvious extension to $\Phi_n(u, u)$, $\Phi_n(B, u)$ and $\Phi_n(B, B)$. In accordance with the generalized energy of the FENE-P model [19, 20], also our shell model has the total energy

$$E \equiv \frac{1}{2} \sum_n |u_n|^2 - \frac{1}{2} \frac{\nu_p}{\tau} \ln \left(1 - \sum_n |B_n|^2 \right). \quad (7)$$

The second term in the generalized energy contributes to the dissipation a positive definite term of the form $(\nu_p/\tau^2)P^2(B)\sum_n |B_n|^2$. With $\nu_p = 0$ the first of Eqs. (5) reduces to the well-studied Sabra model of Newtonian turbulence. We therefore refer the model with $\nu_p \neq 0$ as the SabraP model. As in the FENE-P case we consider $c \equiv \nu_p/\nu_s$ to be proportional to the concentration of polymers. In [9] it was shown that this shell model exhibits drag reduction, and the mechanism for the phenomenon was elucidated. Furthermore, it was shown in [11] that for large enough concentration, the Peterlin function can be disregarded (i.e. $P \approx 1$) and, consequently, the dynamics of the system becomes concentration independent, i.e. we reach the MDR asymptote. This behavior of the Peterlin function is shown in Fig. 3. Following the above finding, we consider below the limiting case in which the concentration is large enough for the Peterlin function to be close to unity, $P \approx 1$. Finally, all the numerical simulations reported in this paper have been performed by using $b = -0.2$, $\nu_s = 10^{-7}$ and a constant energy input given by:

$$F_n = \frac{10^{-3}}{u_n^*} \quad (8)$$

for $n = 1, 2$ and $F_n = 0$ for $n > 2$.

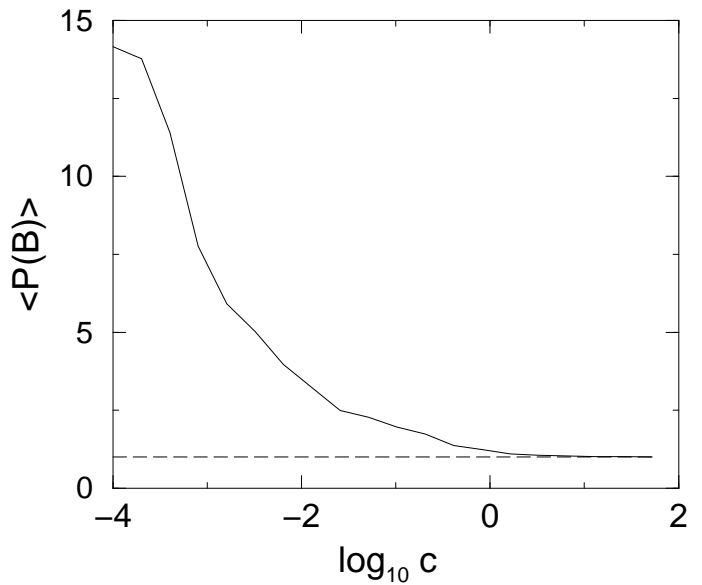


FIG. 3: The average value of the Peterlin function $P(B)$ as a function of c computed in the SabraP model. The dashed line corresponds to $P = 1$.

III. SCALE DEPENDENT EFFECTIVE VISCOSITY IN HOMOGENEOUS DRAG REDUCTION

Drag reduction in homogeneous turbulence is exhibited by a relative increase in the rms fluctuations of the energy at large scales. We thus focus naturally on the energy spectrum $e(k_n) \equiv \langle u_n u_n^* \rangle$. In the context of the shell model the phenomenon is demonstrated in Fig. 2 where $e(k_n)$ is shown for the given values of the parameters. The spectra for the pure Sabra model (line with symbols) and the coupled model (line) are compared for the same amount of power input per unit time. The discussion of the spectra revolves around the typical Lumley scale k_c which is determined by the condition

$$e^{1/2}(k_c)k_c \approx \tau^{-1} \langle P(B) \rangle. \quad (9)$$

For $k_n \gg k_c$ the decay time τ becomes irrelevant for the dynamics of B_n . The nonlinear interaction between u_n and B_n at these scales results in both of them having the same spectral exponent which is also the same as that of the pure Sabra model. The amplitude of the u_n spectrum is however smaller than that of the pure Sabra in the coupled case, since the B_n field adds to the dissipation. On the other hand, for $k_n \ll k_c$ the B_n field is exponentially suppressed by its decay due to τ , and the spectral exponent of u_n is again as in the pure Sabra. Drag reduction comes about due to the interactions at length scales of the order of k_c which force a strong tilt in the u_n spectrum there, causing it to cross the pure Sabra spectrum, leading to an increase in the amplitude of the energy containing scales. This is why the kinetic energy is increasing for the same amount of power input, and

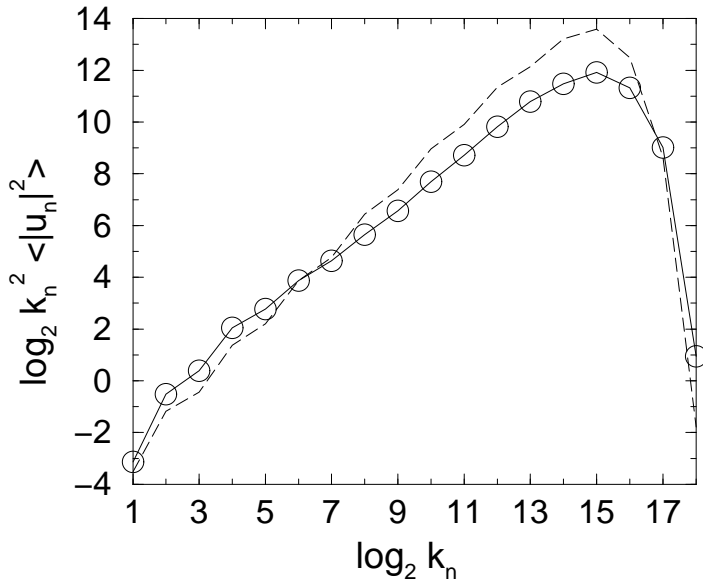


FIG. 4: The spectrum of the energy dissipation $k_n^2 e(k_n)$ for the Sabra (solid line with symbol) and the SabraP models (dashed line). Both models show the same maxima for about $n \sim 15$ which corresponds to the peak in the energy dissipation.

hence drag reduction. In Fig. 4 we show the spectrum of energy dissipation $k_n^2 e(k_n)$. This figure indicates that as far as the dissipative scale is concerned, it is not changed much by the coupling of the velocity field to the polymer field; both models show a maximum at $n \sim 14$ which is the dissipative scale. We now address the question how to recapture the same phenomenon in a model involving the velocity field alone but with a scale-dependent effective viscosity. We first reiterate that the field u_n loses energy in favor of the field B_n . Using Eq. (5) we can measure the energy transfer from u_n to B_n using the quantity:

$$S_p \equiv \sum_n s_p(k_n) \equiv \frac{\nu_p P(B)}{3\tau} \text{Re}\{i \Sigma_n u_n^* \Phi_n(B, B)\}. \quad (10)$$

This function measures the exchange between the kinetic energy $\Sigma_n u_n^* u_n$ and the “polymer” or “elastic” energy $\Sigma_n B_n^* B_n$. In Fig. 5 we show a snapshot of the dependence of the function S_p on time. The point to notice is that S_p is negative for most of the time. The B_n field drains energy from the velocity field, and we therefore can hope to be able to capture its role by an effective viscosity. Note however that the dynamics of S_p is strongly intermittent; this feature is common to the shell model and the full FENE-P model as observed in the DNS of the latter. We cannot hope to capture *all* the temporal complexity with the notion of effective viscosity, since the latter is an average notion. Nevertheless the essential features will be shown to be reproduced. We will try to capture the effect of S_p in terms of an effective viscosity as follows: using $\langle \dots \rangle$ for the (time) average, we introduce the scale dependent effective viscosity $\nu_e(k_n)$

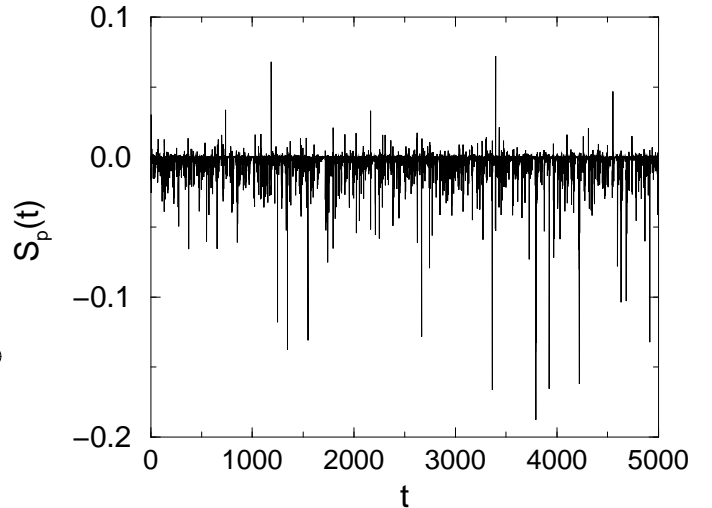


FIG. 5: Time behavior of S_p , as defined in Eq. (10), which represents the whole energy exchange from the u_n field to B_n . Negative values of S_p means that energy is taken from u_n .

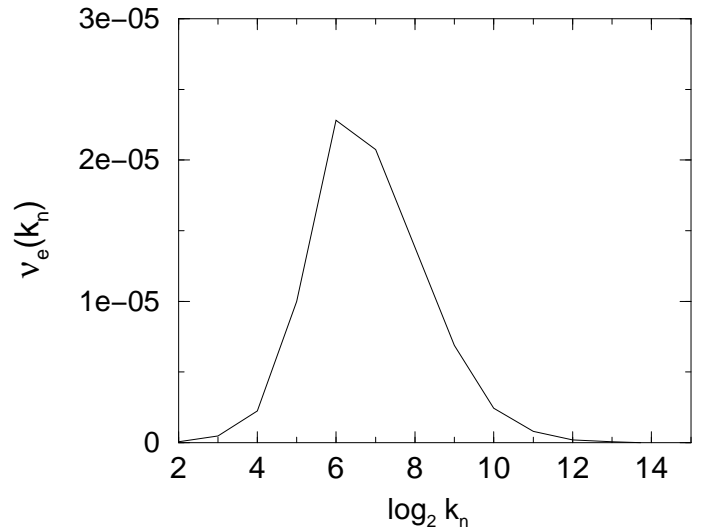


FIG. 6: The values of the eddy viscosity $\nu_e(k_n)$ defined in Eq. (11) for $P(B) = 1$. Note that this quantity rises rapidly in the vicinity of the Lumley scale.

as:

$$\nu_e(k_n) = \frac{\langle s_p(k_n) \rangle}{k_n^2 e(k_n)}. \quad (11)$$

The quantity $\nu_e(k_n)$ is shown in Fig. 6; its maximum is reached at $n \sim 6-7$, a wavenumber which is not yet in the dissipative range. It is important to stress that $\nu_e(k_n)$ is obtained by averaging over a complex and intermittent dynamical behavior of the viscoelastic shell model. It is therefore not obvious that the main characteristics of drag reduction can be obtained by simply replacing the viscoelastic terms $\Phi_n(B, B)$ by a scale dependent effective viscosity. We demonstrate that this is possible by

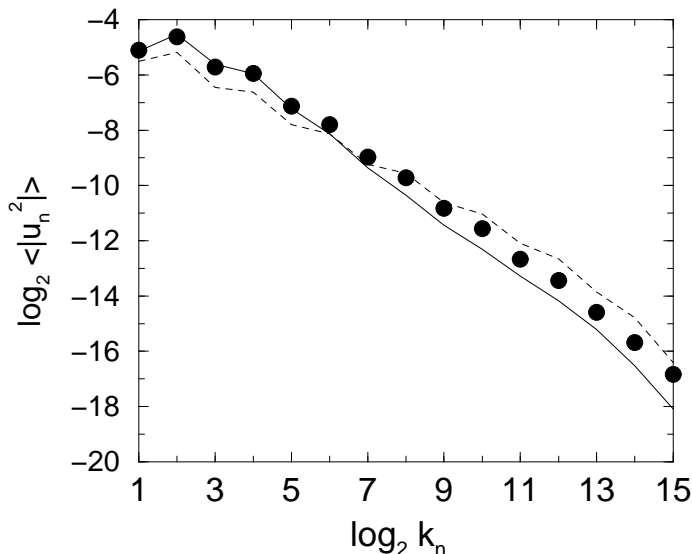


FIG. 7: The energy spectrum of the SabraP model (solid line) as compared with the energy spectrum of the Sabra model with the effective viscosity and $\alpha = 0.3$ (symbols) and the Sabra model without effective viscosity (dashed line).

using now the Sabra model with an extra viscous term given by $\nu_e(k_n)k_n^2u_n$. The new viscous term replaces, on the average, the effect of viscoelastic terms proportional to $\Phi_n(B, B)$. The equations of motion read:

$$\frac{du_n}{dt} = \frac{i}{3}\Phi_n(u, u) - \nu_e(k_n)k_n^2u_n - \nu_s k_n^2 u_n + F_n. \quad (12)$$

We do not expect that $\nu_e(k_n)$ in the *dynamics* of the Sabra model, as proposed in Eq. (12), will be exactly the object measured on the average defined in Eq. (11). We clearly must keep the functional dependence of ν_e on k_n , but we can allow a factor of proportionality that will take care of the difference between the dynamical intermittent behavior and the average behavior. We will therefore use the form $\alpha\nu_e(k_n)$, where α is a constant that can be optimized to achieve a close correspondence between the two-field model and the effective one-field model. For $\alpha = 0$ we recapture the original Sabra model without effective viscosity. We simulated the Sabra model with the effective viscosity [Eq. (12)] for different values of α in the range (0, 1). Drag reduction was found in all cases. For $\alpha = 0.3$ the energy spectrum turns out to be very close to the original SabraP model *with the viscoelastic terms*. In Fig. 7 we show the energy spectrum of the SabraP model and the energy spectrum of the Sabra model with effective viscosity for $\alpha = 0.3$. In order to check that the result shown in Fig. 7 are due to a *scale dependent* dissipation, we have defined a *scale independent viscosity* ν^* as:

$$\nu^* = \frac{\langle S_p \rangle}{\sum_n k_n^2 e(k_n)} \quad (13)$$

The definition of ν^* is similar to that given in Eq. (11), i.e. ν^* is defined such that, by adding a viscous term $\nu^*k_n^2u_n$ to the Sabra model, the system *on the average* is losing the same amount of energy as in the case of viscoelastic flows. It turns out that in our case $\nu^* \sim 2.5 \times 10^{-7}$. By using this value for ν^* we have numerically integrated the Sabra model by adding a new viscosity equal to ν^* , namely:

$$\frac{du_n}{dt} = \frac{i}{3}\Phi_n(u, u) - \nu^*k_n^2u_n - \nu_s k_n^2 u_n + F_n \quad (14)$$

The corresponding energy spectrum is shown in Fig. 8 together with the energy spectrum for the Sabra model (viscosity ν_s) and the Sabra model with the effective viscosity $0.3\nu_e(k_n)$. As one can clearly see, an increase of the dissipation for all scales does not result in a drag reduction. Finally, we have computed the energy flux of the Sabra model with effective dissipation and compared it against the energy flux of the SabraP model. This comparison is exhibited in Fig. 9 where the solid line corresponds to the SabraP model and the symbols correspond to the Sabra model with effective dissipation $0.3\nu_e(k_n)$. The two energy fluxes are equal in the inertial range up to wavenumber $n \sim 7$.

The results illustrated so far support the conclusion that a scale dependent effective viscosity is able to reproduce most of the dynamics of viscoelastic terms and, in particular, the phenomenon of drag reduction. Let us remark once more, that it is the *scale dependence* of the effective viscosity which is able to properly reproduce the drag reduction. It is worthwhile to explain the mechanism of the action of the scale dependent viscosity, to understand its similarity to the action of the polymers. For fixed energy input, as in our case, drag reduction is shown as an increase of the rms fluctuations at scales larger than the Lumley scale. The scale dependent effective viscosity increases the viscous terms $k_n^2u_n$ in a particular range of scales, say for $n_c < n < n_2$, where $n_c = \log_2(k_c)$. The energy flux Π_n in the system is given by the third order correlation function

$\Pi_n \sim \langle u_{n-1}^* u_n^* u_{n+1} \rangle$. As shown in the Fig. 9, we can safely assert that the energy flux does not change for $n < n_c$. The increase of viscosity at $n = n_c$ produces a decrease of the energy at scale n_c . Thus, we expect u_{n_c} to decrease with respect to the value observed in the Newtonian case. Since Π_n is not affected by the increase of the viscosity at $n = n_c$, we must conclude that the quantity $u_{n-1}u_n$ should increase while u_{n_c} decreases. This is the origin of the tilt in the u_n spectrum in the vicinity of n_c . From a physical point of view, this picture is not different from the one discussed in [9] where a similar explanation for the drag reduction was invoked. Note that all that we need for the phenomenon to occur is that the increase in viscosity should start at the right scale. This scale is equivalent of the Lumley scale whose role in the viscoelastic case had been already emphasized.

Finally, we discuss the effect of changing the concentration on the effective viscosity. When $\langle P(B) \rangle > 1$ the ef-

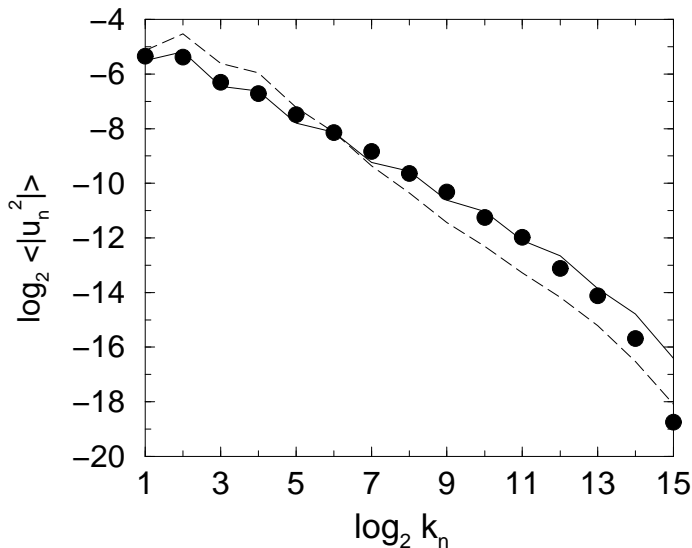


FIG. 8: Energy spectrum of the Sabra model for ν_s (line), the Sabra model with increased viscosity ν^* (symbols) and for the Sabra model with an effective viscosity $0.3\nu_e(k_n)$ (dashed line).

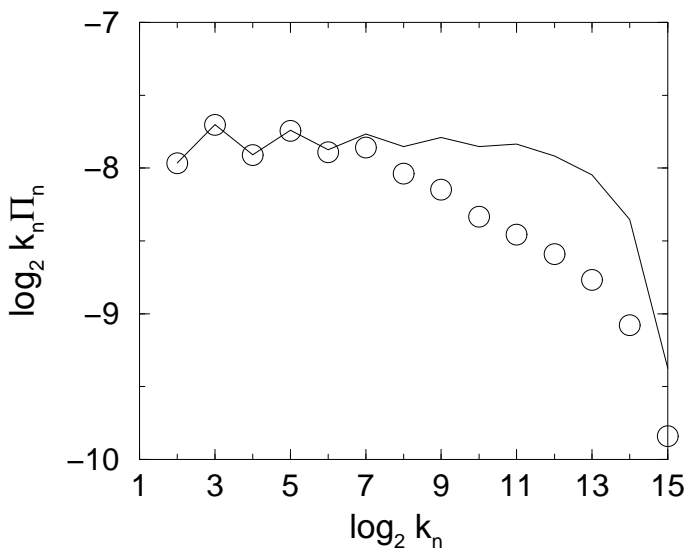


FIG. 9: Energy flux computed for the SabraP model (solid line) and the Sabra model with effective viscosity (symbols).

effective viscosity depends on the Peterlin function, which in turn depends on the concentration c and on the relaxation time τ , cf. Eq. (11). Figure 10 displays the effective viscosity as a function of k_n for four values of the concentration, $c = 10^{-2}$, 10^{-1} , 10 and 100 . As the concentration decreases, the effective viscosity decreases, and its peak migrates to higher values of k_n . This migration is simply due to the change in the Lumley scale, cf. Eq. (9). The decrease in the effective viscosity is due to the increase in $\langle P(B) \rangle$ shown in Fig. 3. Needless to say, these changes in the effective viscosity decrease the

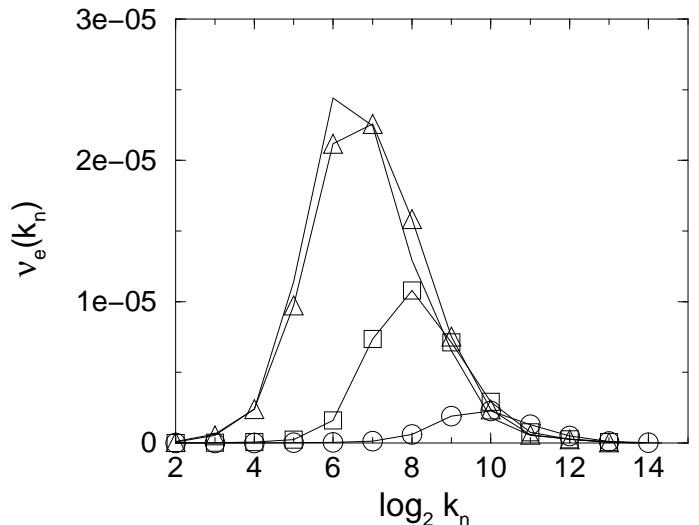


FIG. 10: Effective viscosity for varying the concentration: $c = 10^{-2}$ (circles), $c = 10^{-1}$ (squares), $c = 10$ (triangles) and $c = 100$ (line).

effect of drag reduction, as seen in experiments and simulations: only large concentrations agree with the MDR asymptote.

IV. THE LIMIT OF LARGE SYSTEM SIZE

In this section we want to discuss the limit $k_0 \rightarrow 0$ while keeping fixed the scale and the shape of the effective viscosity. In other words, we study $k_0 \rightarrow 0$ for fixed value of the Lumley scale k_c . Note that we take k_c much smaller than the dissipative scale and we keep constant the rate of energy input ϵ .

The discussion simplifies by considering the other typical scale in our system, which is the Taylor microscale λ_T ,

$$\lambda_T \equiv \sqrt{\frac{\sum_n \langle |u_n|^2 \rangle}{\sum_n k_n^2 |u_n|^2}}. \quad (15)$$

In [9] it was shown that the conditions are optimal for drag reduction in our shell model when a dimensionless parameter $\mu \equiv \lambda_T k_c$, is of the order of unity. On the other hand drag reduction is lost when $\mu \gg 1$ or $\mu \ll 1$. Obviously, when $k_0 \rightarrow 0$ the overall kinetic energy increases as $k_0^{-2/3}$ while the denominator in Eq. (15) remains unchanged, being dominated by the viscous scale. Thus $k_0 \rightarrow 0$ leads to $\lambda_T \rightarrow \infty$, and we expect to lose drag reduction in that limit (for a fixed value of k_c). This conclusion is supported by the results shown in Fig. 11, where we plot the ratio between the kinetic energy with the effective viscosity and the Newtonian kinetic energy for $L \equiv k_0^{-1} \rightarrow \infty$. The case $L = 1$ corresponds to the previous sections. Note that for L large enough, the system exhibits drag enhancement. Physically, for very large

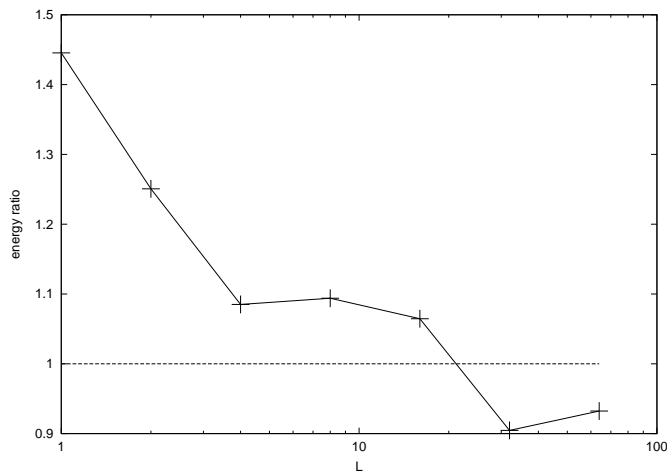


FIG. 11: Ratio of the kinetic energy for the Sabra model with scale dependent viscosity and the kinetic energy of the Sabra model with fixed kinematic viscosity, for different values of $L \equiv k_0^{-1}$. Note that for drag reduction to take place the ratio must be larger than 1. The position the maximum in the scale dependent viscosity is kept fixed while $L \rightarrow \infty$.

values of k_c/k_0 the effective dissipation is just increasing the overall viscosity in the system and, therefore, no drag reduction can be observed. For drag reduction to occur we must have the Lumley scale close to energy containing scales. Note, however, that “close” in our case means $k_c \sim 50 - 100$ larger than the integral scale k_0 .

It is interesting to compare our findings, which pertain to homogeneous systems, to drag reduction in turbulent boundary layers. The elastic layer in such flows (between the viscous layer and the Newtonian plug) has the peculiar distinction that y , the distance from the wall, becomes the only important scale in the problem. It is both the energy containing scale and the Lumley scale at the same time. The former is clear; at distance y from the wall the most energetic eddies are of size y . The latter needs a bit of theory, and this is provided in [18]. The upshot of the analysis there is that in the elastic layer the kinetic energy $K(y)$ scales like $K(y) \sim y^2/\tau^2$. Thus the Lumley scale is also y . Accordingly, the phenomenon of drag reduction is totally indifferent to the physical size of the channel (or pipe). As long as the conditions for drag reduction hold at distance y from the wall, drag reduction will occur and will have a persistent effect on the mean flow independently of the outer scale. Eventually, when y is large enough, $K(y)$ may stop growing like y^2 , the Lumley scale decreases, and we observe cross over back to the Newtonian log layer, albeit shifted to a larger value of a mean velocity profile.

In summary, drag reduction phenomena in homogeneous and wall bounded flows have a lot in common even though the effect disappears in the former when the system size goes to infinity. The essential physics is the proximity of the Lumley scale to the energy containing scales, which allows an effective interaction between the

polymer dynamics and the hydrodynamic modes.

V. CONCLUSIONS

The work presented in this paper supports two conclusions. First, we demonstrated that drag reduction by polymers can be represented in terms of an effective scale dependent viscosity. One can use a theory in which two fields are explicitly presented, i.e. the velocity field and the polymer field. Then the viscosity remains Newtonian, and the polymer conformation tensor acts as the additional sink of energy at the intermediate scales which are larger than the viscous scales but smaller than the Lumley scale. We can construct however effective models in which only the velocity field is present, and replace the polymer field by an effective viscosity. This effective viscosity will be different from the Newtonian one at the crucial scales at which the polymers are active, i.e. scales larger than the dissipative scales but smaller than the Lumley scale. With a properly chosen effective viscosity we can reproduce the results of the two-field theory qualitatively and even semi-quantitatively. Having done so, we reach a unified discussion of drag reduction by polymers in homogeneous and wall bounded flows. It is worth pointing out however that the unified discussion is deeper than the device of unified viscosity. Superficially drag reduction in homogeneous and wall bounded turbulence appear very different. In the former there is no mean flow and drag reduction appears as an increase of the rms fluctuations of the large scales. In the latter drag reduction means the increase of the mean flow velocity. Nevertheless in essence the phenomenon of drag reduction in homogeneous and wall bounded flows is basically the same: the polymers act to reduce the gradients at the intermediate scales. They partly laminarize the flow at the intermediate scales, and this allows the largest scales to attain higher rms fluctuation levels (in homogeneous flows) or higher mean velocity (in wall bounded flows). To understand this further recall that for laminar flows the drag is a strongly decaying function of Re. Once turbulence sets in, the dramatic increase in eddy viscosity contributes to a drag which is much larger than the one that would obtain in a hypothetical laminar flow with the same value of Re. The addition of polymers allows one to bring the drag closer to the hypothetical laminar low value, and this is done by reducing the turbulence level at intermediate scales. Whether one prefers to describe the quantitative aspects of this phenomenon using explicitly the polymer field or by employing an effective viscosity depends to a large extent on one’s goals. We expect that the concept of effective viscosity will be found equally useful in discussing drag reduction in other situations, for example when microbubbles are used instead of polymers. The quantitative aspects of such a description need however to be worked out case by case, and this is our program for the near future.

Acknowledgments

This work was supported in part by the European Commission under a TMR grant, the US-Israel Bina-

tional Science Foundation, and the Minerva Foundation, Munich, Germany. ESCC was supported by a grant of the Research Grant Council of Hong Kong (Ref. No. CUHK 4046/02P).

-
- [1] K. R. Sreenivasan and C. M. White, *J. Fluid Mech.* **409**, 149 (2000).
- [2] J. L. Lumley, *Ann. Rev. Fluid Mech.* **1**, 367 (1969)
- [3] P.S. Virk, *AIChE J.* **21**, 625 (1975)
- [4] P.-G. de Gennes *Introduction to Polymer Dynamics*, (Cambridge, 1990).
- [5] B.A. Toms, *Proc. 1st Intl. Congress on Rheology*, vol. 2, 135 (North Holland 1949).
- [6] J.M.J de Toonder, M.A. Hulsen, G.D.C. Kuiken and F. T.M Nieuwstadt, *J. Fluid. Mech* **337**, 193 (1997).
- [7] C.D. Dimitropoulos, R. Sureshdumar and A.N. Beris, *J. Non-Newtonian Fluid Mech.* **79**, 433 (1998).
- [8] E. de Angelis, C.M. Casciola and R. Piva, *CFD Journal*, **9**, 1 (2000).
- [9] R. Benzi, E. De Angelis, R. Govindarajan and I. Procaccia, *Phys. Rev. E* **68**, 016308 (2003).
- [10] R. Benzi and I. Procaccia, *Phys. Rev. E* **68**, 025303 (2003).
- [11] R. Benzi, E. Ching, N. Horesh, I. Procaccia, "Theory of concentration dependence in drag reduction by polymers and of the MDR asymptote", *Phys. Rev. Lett.* submitted (2003).
- [12] E. De Angelis, C.M. Casciola, V.S. L'vov, R. Piva and I. Procaccia, *Phys. Rev. E*, **67** 056312 (2003).
- [13] bottle neck
- [14] R. Govindarajan, V.S. L'vov and I. Procaccia, *Phys. Rev. Lett.*, **87**, 174501 (2001).
- [15] R. Govindarajan, V. S. L'vov and I. Procaccia, "Stabilization of Hydrodynamic Flows by Small Viscosity Variations", *Phys. Rev. E*, submitted.
- [16] S. B. Pope, *Turbulent Flows* (Cambridge, 2000).
- [17] M.V. Zagarola and A.J. Smits, *Phys. Rev. Lett.* **78**, 239-242 (1997).
- [18] V.S. L'vov, A. Pomyalov, I. Procaccia and V. Tiberkevych, *Phys. Rev. Lett.*, submitted.
- [19] R.B. Bird, C.F. Curtiss, R.C. Armstrong and O. Hassager, *Dynamics of Polymeric Fluids* Vol.2 (Wiley, NY 1987)
- [20] A.N. Beris and B.J. Edwards, *Thermodynamics of Flowing Systems with Internal Microstructure* (Oxford University Press, NY 1994).
- [21] B. Yu, Y. Kawaguchi, S Takagi and Y. Matsumoto, The 7th symposium on smart control of turbulence, University of Tokyo, March 2001.